ISEIS

Journal of Environmental Informatics 24(2) 65-79 (2014)

Journal of Environmental Informatics

www.iseis.org/jei

Assessing the Impacts of Future Urban Development Patterns and Climate Changes on Total Suspended Sediment Loading in Surface Waters Using Geoinformatics

Y. C. Jordan[1], A. Ghulam[1,*] and M. L. Chu[2]

[1]*Center for Sustainability at Saint Louis University, St. Louis, Missouri 63108, USA*
[2]*Agricultural and Biological Engineering, University of Illinois, Urbana-Champaign, Illinois 61820, USA*

Received 3 December 2012; revised 30 November 2013; accepted 16 March 2014; published online 20 November 2014

ABSTRACT. Water pollution is a major global issue that has profound impact on sustainable development of our society. In this paper, land cover change trajectories of the study area over the last three decades are developed using Landsat data. Then historic land-cover and land-use change (LCLUC) patterns are used to estimate, calibrate and validate key drivers of land use change. Future likelihood of land-cover/land-use for 2021 and 2031 are simulated using state-of-art image processing techniques based on the driving factors of land use change integrated with Land Change Modeler. Hypothetical scenarios of LCLUC including a) low density of new urbanization growth and open land with vegetation cover, b) normal urbanization and, c) highly development of commercial/urban land use and impervious surfaces, are constructed during the simulations. The Soil and Water Assessment Tool (SWAT) is employed to generate total suspended sediment with the various combinations of three hypothetical scenarios mentioned above and climate change scenarios projected for 2021 and 2031. The future climate patterns for the periods of 2011-2021 and 2021-2031 are generated from the intergovernmental Panel on Climate Change (IPCC) Spatial Report for scenarios A1B, B1, and A2. A total of 19 SWAT models are generated, one for 2011, nine for 2021 and 2031 respectively. The results are then used to compare and identify the impacts of combined land use and climate change on surface water quality, to answer and confirm the hypothesis that urban sprawl developing patterns in the greater St. Louis region have significant impacts on surface water quality in specific way.

Keywords: land-cover and land-use change, remote sensing, water pollution, St. Louis metropolitan area

1. Introduction

Based on the sources of pollutants, water pollution is categorized as point-source and nonpoint source pollution. Unlike point-source pollution, caused by industrial and sewage treatment plants, nonpoint source pollution is caused by rainfall or snowmelt moving overland and through the ground which deposits natural and manmade pollutants on the surface and into the ground water (Callan and Thomas, 2012). Urban development influences the timing and magnitude of runoff as the impervious surface area increases (Randhir and Hawes, 2009). Consequently, the urban development increases the nonpoint source pollutants loading into the surface water (Dissmeyer, 2000; Phillips and Lewis, 1995). Suspended sediment is one of the major pollutants associated with urban runoff (Deletic, 1998; Sonzogni et al., 1980). Pimentel (2000) reported that more than 60 percent of water-eroded soils in the United States load into surface waters. Studies of the movement of chemical contaminations in soils with the conversion of permeable areas to impermeable urban land cover show that urban expansion is associated with high loading of nonpoint source contaminants in nearby surface waters (Callender and Rice, 2000; Dierberg, 1991; Frumkin, 2002; Van Metre et al., 2000). Numerous studies have shown that water quality is negatively affected by surface runoff increase and nonpoint source pollution loading caused by urban developing or by land-cover and land-use changes (LCLUC) (Dreher and Price, 1992; Goonetilleke et al., 2005; Ierodiaconou et al., 2004; Weng, 2001; Wilson and Weng, 2011; Young et al., 1996).

Urban development raises a number of pressures on waterways because the development affects runoff and hence the water balance in catchments (Leopold, 1968; Stephenson, 1994). As the vegetation cover and open areas are reduced and impervious surfaces are increased, rainfall less likely to infiltrate through soils and returned to ground-water aquifers, and instead more commonly flows as stormwater runoff to streams and rivers (Noble, 1999). The impervious surfaces created by large expanses of pavement and concrete increase the volume and rate of runoff during the storm time. The reconfiguration of the landscape during the urban development, such as clearing and moving of soil increases erosion and leads to sedimentation and excess turbidity of waterways. As a result, wash outs of "cultural pollutants" (e.g., abandoned properties) and impervious surfaces in the urbanized en-

* Corresponding author. Tel.: 314-977-5156.
E-mail address: awulamu@slu.edu (A. Ghulam).

ISSN: 1726-2135 print/1684-8799 online
 doi: 10.3808/jei.201400283

vironment may have increased sedimentation and pollutant concentration in surface water. The longstanding phenomenon of rapid expansion of suburban areas at the cost of shrinking metropolitan regions with a complex pattern of LCLUC, transportation, social and economic developments has been defined as "urban sprawl" (Frumkin, 2002). Urban sprawl is one of the major forces driving LCLUC in the United States (Hasse and Lathrop, 2003). There is evidence that urban sprawl contributes to water pollution in certain specific ways (Frumkin, 2002), but further evidence is needed to identify the precise features of LCLUC that best predict nonpoint source pollution in the urban sprawling metropolitan regions.

Undoubtedly, the impacts of suburbanization and depopulation in the urban core on water quality have been further exacerbated by increased frequency and intensity of rainfall projected over the Midwest (IPCC, 2007; Pan et al., 2004). There have been a large number of publications in the literature concerned about the impacts of climate change on the water resources (Burn, 1994; Caballero et al., 2007; Frederick and Schwarz, 1999; Fu et al., 2007; Jyrkama and Sykes, 2007; Mortsch and Quinn, 1996; Nunes et al., 2009; Scibek and Allen, 2006; Thomas et al., 2007; Xiong et al., 2009). Multiple studies have investigated the impacts of future climate scenarios generated from Global Climate Model (GCM) on the water resources by using the Soil and Water Assessment Tool (SWAT). For example, Stone et al. (2003) found that the water yields were dramatically increased for the doubled CO_2 scenarios compared to the historical climate; Arnell (2005) found that different climate scenarios could cause big fluctuations in runoff; Jha et al. (2004a) suggested that the future climate would cause a large increase in streamflow; Abbaspour et al. (2009) projected more frequent and larger-intensity floods in wet regions and more prolonged droughts for dry regions. However, water quality issues in metropolitan urban areas are complex, which requires numerous case studies based on thorough understanding of historic and future incentives of urban planning, population dynamics and patterns of hydrologic systems. It is pivotal to integrate the climate change with LCLUC to assess its interactive effects on water quality in urban or metropolitan region (Clifford, 2009). Efforts on simulating the water quality outcomes of combined climate change and LCLUC studies may be exemplified by a number of reports (e.g., Chang, 2003, 2004; Chen et al., 2005; Choi, 2008; Davis Todd et al., 2007; Ducharne et al., 2007; Franczyk and Chang, 2009; Mimikou et al., 2000; Samaniego and Bardossy, 2006; Wilby et al., 2006; Wang et al., 2005). There are very few studies focused on the coupled impacts of simulated future LCLUC and climate change scenarios on the runoff and water quality. Franczyk and Chang (2009) examined the relative importance of future climate and LCLUC in controlling the quantity and quality of water resources in the sub-basin scale while Wilson and Weng (2011) simulated the impacts of future LCLUC and climate changes on surface water in both watershed and subbasin scales. While these studies all indicated that climate change and future LCLUC has a significant influence on basin hydrologic response, the authors acknowledged that their findings were preliminary, and therefore, more knowledge is needed in different natural and urbanized human environments to reach a more generalized conclusion. The issue of the complicated scenarios of future LCLUC and climate change is at the crux of a central problem in predicting its possible impacts on water quality, which is the inability to generalize across studies over different geographic regions. Different case studies and applications are essential to test similar methods so as to generalize preliminary results in both space and time with comparative examples (Ingram et al., 2005; Woodcock et al., 2001).

The growing number of water pollution problems plus budgetary constraints particularly at today's harsh economic times requires scientific understanding of the causes and patterns of water quality deterioration to ensure innovative solutions and developing effective water management practices. The overarching goal of this research is to determine the impacts of future urban developing or LCLUC patterns on total suspended sediment (TSS) loading into surface waters under different climate change scenarios, and to identify the sustainable development strategies targeted at reducing the suspended sediment contaminant to the surface waters. Specifically, this study is aimed to compare the effects of future land use changes combined with different climate projection scenarios to the TSS loading rate to stream flows. This study presents a unique approach, unlike other previous studies (e.g. Wang et al., 2005) by applying a conceptual distributed hydrological model SWAT with series of climate change scenarios and future land change simulations based on remote sensing data integrated with socioeconomic variables including crime, distance to work, and strategic plan for economic development.

2. Study Area

The study area is located at the confluence of three mighty rivers: the Illinois, Missouri, and Mississippi Rivers (Figure 1). Water quality has become an issue of increasing concern in the region due to the impact of LCLUC, particularly from the increased pressure of suburbanization accompanied by continuous depopulation of the inner urban center, leaving behind crumbling infrastructures. The Mississippi River flows from the north and first meets the Illinois River, and then joins the Missouri River. The St. Louis metropolitan region located on the Mississippi River just below the point where it meets the Missouri River, is at the heart of the study area. This intersection of the major American waterways established the reputation of "Gateway to the West" for St. Louis. From the early 18th century, people have started being attracted by this confluence and its abundant resources, and settling down on this fertile land to create their lives and community, or launched their new journeys from here, such as Lewis and Clark (Committee on Missouri River Ecosystem Science and National Research Council, 2002). Like most other older metropolitan areas, St. Louis is experiencing an urban sprawl type of development pattern, it's suburbs are spreading out over more and more rural land at the periphery of urban area (Frumkin, 2002; Hasse and Lathrop, 2003) while the population in the urban core is shrinking. People moved from the cities and migrated into the

surrounding suburbs to build up their homes on a larger land lot, to pursue safe, quiet, and private life style.

The City of St. Louis is the third largest metropolitan city on the Mississippi River floodplain. As a typical post-industrial city that once served as an industrial powerhouse in the Midwest but in recent years has entered a period of steep decline with greater concentration of poverty, the city population has shrunk from its peak in 1950 of 856,796, to 319,294 as recorded in the 2010 census, having lost 8.3% of its population since 2000. The city population has been steadily moving further out of the city limits as a result of crumbling infrastructure, increased crime, failing urban schools (Immergluck, 2010), and a self-perpetuating cycle of disinvestment. Recent studies show that while greater urban areas have increased by 43% over the last two decades in the Greater St. Louis region, both the population within the city limits and overall vegetation cover has declined (Jordan et al., 2012).

The climate of the study area is continental type with distinct alteration of seasons characterized by wide ranges in temperature, and irregular annual and seasonal precipitation. In the summer time, the moist and warm air masses blown from the Gulf of Mexico bring abundant rainfall for this region. According to the climatology and weather records from the National Weather Service Weather Forecast Office, from 1874 to present, the highest and lowest annual rainfall in this area was recorded as 1472.2 mm (year 2008) and 522.2 mm (year 1953), respectively. Usually the rainy season is distributed from May to August. The elevation of surface topography ranges from 68 m at Chester to 530 m at the hilly area of the south-west St. Louis County. The land of Missouri and Illinois in this region is lying on a karst geomorphologic setting that can trigger the intense relationship between surface and groundwater (Criss and Wilson, 2003). The main land use categories in the area are forest, followed by agriculture and pasture, then by urban. The major crops are soybeans, corn, and wheat, and the major forest is dominated by deciduous oak-hickory forest.

3. Materials

3.1. Land-cover and Land-use Data

Historical land-cover and land-use (LCLU) images of 1992 and 2001 were obtained from National Land Cover Database (NLCD, 2012) while the LCLU maps of 2011 were generated by remote sensing data. Three clear sky Landsat Thematic Mapper (TM) images cover the study area were collected in October, 2011. Radiometric calibrations and atmospheric corrections were performed to derive surface reflectance using QUick Atmospheric Correction (QUAC) (Bernstein et al., 2005) available with ENVI® image processing and analysis software from EXELIS Visual Information Solutions.

3.2. Watershed Data

10-m digital elevation data was obtained from United States Geological Survey national elevation dataset (USGS, 2012a) for watershed delineation and slope calculation. Stream flow data were solicited from USGS archival station discharge database (USGS, 2012b) and U.S. Army Corps of Engineers (USACE) database. TSS data corresponding to the monitoring stations shown in Figure 1 were acquired from USGS database (USGS, 2012b) and Illinois Environmental Protection Agency database (EPA). Water use data were obtained from Water Resources Center of Missouri Department of Natural Resources (MDNR, 2012).

Our focus in the paper is to understand TSS loading rate under various future scenarios of land use and climate changes. To that end, future stream flows for the inlets were projected based on the historical data using autoregressive moving average time series models (Box and Jenkins, 1970; Tiao and Box, 1981) given by:

$$X_t = c + \varepsilon_t + \sum_{i=1}^{p} \varphi_i X_{t-i} + \sum_{i=1}^{q} \theta_i \varepsilon_{t-i} \quad (1)$$

where X_t is the time series data, c is a constant, ε_t are white noise error terms, φ_i are the parameters of the autoregressive part of the model, and the θ_i are the parameters of the moving average part.

3.3. Climate Data

Climate data from 1900 to present were collected from National Environmental Satellite Data and Information Service (NESDIS) (NOAA, 2012), which include data collected over 43 precipitation and 23 minimum and maximum temperature stations. Inverse Distance Weighted (IDW) method was applied to spatially interpolate missing precipitation and temperature data using SPELLmap (USDA, 2012). Future climate data were obtained from World Climate Research Program's (WCRP'S) Coupled Model Inter-comparison Project Phase 3 (CMIP3) multi-model dataset (Liang et al., 2012; Maurer et al., 2007).

4. Methods

4.1. LCLUC Prediction

Appropriate land use change datasets and analytical tools are needed to understand and monitor the patterns and processes involved in the phenomenon of urbanization. Future LCLU cover scenarios were simulated using Land Change Modeler (LCM) (Wilson and Wang, 2011). LCM is a land change model that operates on change analysis and prediction, such as generating change maps, uncover underlying trends of complex change, and model transition potentials.

4.1.1. Land-cover Classification

An Iterative Self-Organizing Data Analysis Technique (ISODATA), unsupervised clustering classification method for

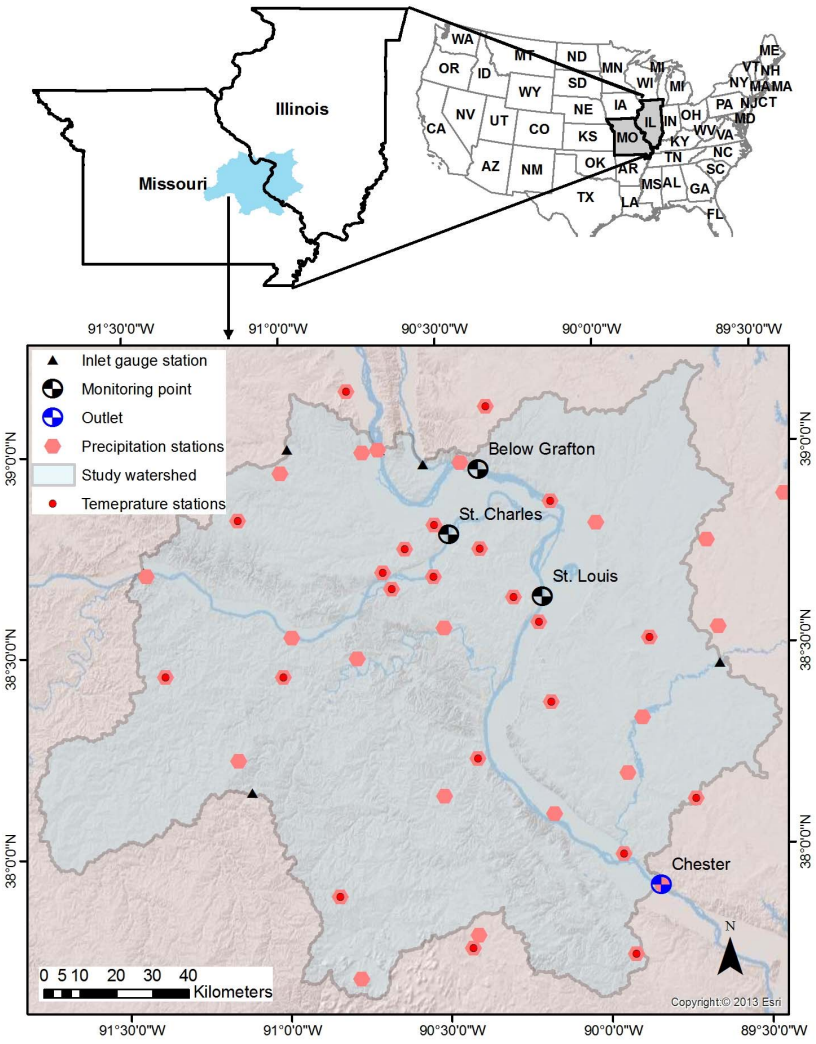

Figure 1. A map showing the location of the study area in St. Louis Metropolitan region, distribution of weather stations, and water gauging stations.

Landsat TM data, was used as the core land cover mapping approach (Jensen, 1996). The ISODATA clustering algorithm compares the radiometric value of each pixel with predefined number of cluster attractors, aggregates pixels in clusters and shifts the cluster mean values in a way that the majority of the former aggregated pixels belongs to a cluster (ERDAS, 1999; Manakos et al., 2000). We set the number of clusters to 100 with 500 iterations. Using our expert knowledge, database of historic land cover dataset, aerial photographs and Google-Earth, we assigned class names to the clusters. Clusters representing the same land-cover types were merged and generalized. The classification accuracy was estimated at 75% by using over 200 sample sites and systematic comparison with Google Earth, which is comparable to National Land Cover Dataset generated by USGS.

Based on the level I categories of the modified Anderson Land Cover classification system (Anderson et al., 1976), the whole study area were categorized into ten classes: Open water (WATR), Low density urban (URLD), Medium density urban (URMD), High density urban (URHD), Barren land (SWRN), Forest (FRSD), Range land (RNGE), Pasture land (HAY), Agriculture land (AGRR) and Wetland (WETF).

4.1.2. LCM Calibration and Validation

LCM was applied to the whole study area to create future LCLU maps for 2021 and 2031. The land cover classification

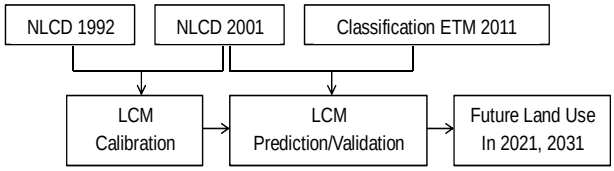

Figure 2. The flow chart of prediction in Land Change Modeler.

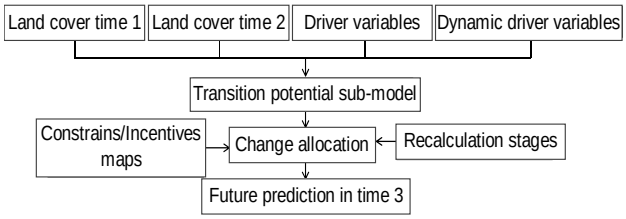

Figure 3. The logic of land cover change prediction in Land Change Modeler is using two land cover maps from time 1 and time 2 to predict what the land cover will be in the future or in time 3.

maps of 1992 and 2001 were used as observed data to calibrate the model, and the classification map of 2011 was used to verify the simulated map for 2011 (Figure 2). The logic of land cover change prediction in Land Change Modeler is shown in Figure 3.

The prediction function of LCM is generated using regression analysis and a Multi-Layer Perceptron (MLP) neural networks which is built on Markov-chain technique. Regression analysis is used to estimate the correlation between LCLUC and population change or other socio-economic variables in the model (Hepinstall et al., 2008; Lopez et al., 2001). Stochastic Markov-chain technique is applied for transition potential model (Figure 3) (Lopez et al., 2001; Wu et al., 2006). Markov chain represents the dynamic transition probabilities of a single class or a group of classes which are supposed to have the same underlying driver variables, described as symmetric matrices (Luenberger, 1979; Wilson and Weng, 2011). For urbanized land cover change, the subsequent cover type is determined by the previous cover type and land use strategy but not the same status as previous, and this change is possible to develop into various different statuses during the developing period (Weng, 2001).

$$\underline{P} = \left[P_{ij} \right] = \begin{bmatrix} P_{11}, & P_{12}, & \ldots & P_{1n} \\ P_{21}, & P_{22}, & \ldots & P_{2n} \\ P_{31}, & P_{32}, & \ldots & P_{3n} \\ P_{n1}, & P_{n2}, & \ldots & P_{nn} \end{bmatrix} \quad (2)$$

In the equation, $P = [P_{ij}]$ represents the probability of transitioning from the previous state i to the subsequent different state j or to multiple states ($i1$, $i2$, …, ij) as depicted by the matrix.

The driver variables, constraints/incentives, applied in the model include the evidence likelihood of change in previous time, land value, crime level, the distance from the City of St. Louis, the distance to stream, and elevation. Evidence likelihood is an empirical probability of change between the land use images in the previous time and the later time (Wilson and Weng, 2011).

A total of 41 transitions occurred within the study area during 2001 to 2011 while the areas of changes were smaller than 1 km^2 was ignored because of the process limitation of LCM on transition number. Each of transitions was modeled separately in LCM to achieve their change potentials, and prediction image was created by MLP procedure based on the potentials. In the final process, three sets of land use maps, were generated for 2021 and 2031 based on three future land use scenarios: (1) low density urban incentive scenario (LI) encouraged a low density of new urbanization growth and open land with vegetation cover; (2) historical trend incentive scenario (MI) encouraged the normal urbanization patterns respond to the LCLUC drivers in the historical trend of land cover changes; (3) high density urban incentive scenario (HI) was highly encouraged to the development of high density comercial/urban land use and impervious surfaces. During the modeling process, incentives were given to the encouraged classes, and all other land use classes were set as normal parameters. The incentives given to the future LCLUC scenario was equal to twice the 10-year trend of the historic change rate. For example, if the growth rate of low density urban area is 1% from 2001 to 2011, the 2% incentive was given to the growing rate from 2011 to 2021.

4.1.3. Indicators of Urban Sprawl to Land Resource

Urban sprawling patterns impact on many social and environmental aspects that need to be quantified and related to the water quality. We use the Land Resource Impact (LRI) indicators developed by (Hasse and Lathrop, 2003) to quantify the urban sprawling patterns. This series of five indicators can be used to examine and analyze significant specific land resource impacts to water resources problems attributable to sprawling urban growth. These indicators include: (1) low density of new urbanization; (2) loss of prime farmland; (3) loss of natural wetlands; (4) loss of forest; and (5) increase of impervious surface.

4.2. Future Climate Scenarios

The future climate data for the periods of 2011 ~ 2021 and 2021 ~ 2031 were obtained from the intergovernmental Panel on Climate Change (IPCC, 2000) Spatial Report for scenarios A1B, B1, and A2. A1B is a state of possible rapid economic growth, because of the spread of new and efficient technologies, all energy sources are used in a balance. B1 is possible state that the rapid economic growth as in A1B, but more clean and resource efficient technologies will be introduced to the world. A2 is characterized by independently operating and self-reliant nations in the world with higher

CO_2 emissions (IPCC, 2000).

4.3. SWAT Model Description and Performance Evaluation

The hydrologic response of the watershed under future land use and climate scenarios was simulated using SWAT. The intercombinations of three climate scenarios and three LCLUC scenarios in 2021 and 2031 generated 18 SWAT model simulations. Results showed that TSS has different responses to the conditions with different combinations of climate and LCLUC scenarios.

4.3.1. Theoretical Description of SWAT

SWAT model was applied to generate stream flow and TSS at 10-year interval. This model is a watershed-scale water quality model that operates on a daily time step and is capable of simulating the impacts on water, sediments and chemical yields of detailed land used and land management operations (Arnold et al., 1998). In SWAT, the basic calculation unit is hydrologic response unit (HRU) that consist of homogeneous land use, management, and soil characteristics. The watershed is usually divided into multiple sub-basins, and further subdivided into HRUs (Jha et al., 2004b). Flow, sediment, and non-point source loadings from each HRU are summed, and the resulting loads are routed through channels to the watershed outlet (Arnold et al., 2010; Jha et al., 2004b; Jha, 2011). The components of running SWAT in this research include HRUs information (Singh and Xu, 2006), such as land cover, elevation, soil, precipitation, temperature, stream flow, sediment and nutrient delivery. From the output provided by SWAT, we can derive time series of stream flow and TSS.

4.3.2. SWAT Calibration and Validation

Model calibration and validation were carried out in SWAT by adjusting the stream flow and TSS parameters. The model was calibrated from 2000 to 2005 and validated from 2006 to 2011 using monthly river discharges and sediment loading rate at four gauging stations (see Figure 1): St. Charles, Below Grafton, St. Louis, and Chester. It is worth noting that land cover data of 2001 was used as input for 2000 land use assuming that land use changes within a couple of years are negligible over a landscape. Land cover change rate between 2000 and 2011 was generated using the difference between 2001 and 2011 land cover maps. First, an automatic sensitivety analysis was performed to identify the sensitivity calibration parameters. Then the sequential Uncertainty Fitting program (SUFI-2) (Abbaspour et al., 2004, 2007) was used to automatically calibrate and find out the most optimum value of the sensitivity parameters. Model calibration was performed using monthly time steps from 2000 ~ 2005. The model was then validated from 2006 to 2011. Model performance was evaluated using Nash-Sutcliffe efficiency coefficient (Nash and Sutcliffe, 1970).

Different combinations of three LCLUC patterns and three future climate scenarios generate 18 new future scenarios, nine for 2021 and 2031, respectively (Table 1). The new scenarios were named after the projected emission scenarios and the corresponding future land use simulations. For example, A1BLI scenario uses combination of A1B emission scenario with LI land use change scenario.

In order to identify the emission scenario inducing the highest TSS loading rate, we divided the 18 models into three land use scenario groups, such as: LI group, MI group, and HI group. The effects of each future climate scenario were compared by taking the difference between each two scenarios using the same land cover projection (see Table 1) in the 2021 and 2031, respectively. After that, the subbasin level TSS loading rates of each two models were inter-compared by subtracting one from the other. For example, TSS of A1BLI subtracted by A2LI provides which emission scenario introduced the highest TSS loading. Similar method was applied for identifying the LCLUC scenario relating to the highest TSS loading, but the 18 models were divided into three climate emission scenario groups, and the TSS loading between each two LCLUC scenarios for each group were inter-compared. For example, in order to quantify the degree of difference in TSS between A1B and A2 under the LI land cover group, the TSS simulated using A2 rainfall pattern was subtracted from the TSS simulated using A1B pattern. The results were then summarized in a map called A1BLI-A2LI (Fig. 4a). Similarly, in order to quantify the degree of difference in TSS due to land cover changes, the difference between two land cover scenarios under the same climate projection was computed.

5. Results and Discussions

5.1. Land-use Change Analysis from 2011 and 2031

The LCM models indicated that the study area will experience dynamic changes from 2011 to 2031. The predicted change trajectory between 2011 and 2031 is amplified trend of 2011 to 2021 except slightly different gains and losses rate among LCLU categories in different scenarios (Table 2). These differences exist because of the application of constrain and incentive policy applied in LCM model.

The quantification of LCLU changes for the analyzed categories from 2001 to 2021 and from 2021 to 2031 is in Table 2. Forest, the most extensive land cover type occupies the majority of the study area shows significant loss throughout the study period. The lost in forest area is mainly devoted to LI urban, agricultural land and range land with grasses. Agricultural land is the second decreasing category after forest. LI urban is also the dominant contributor to agriculture land lost. The LI urban experienced the greatest growth from 2021 to 2031. One of the major reasons for this may be sprawl urban development due to population growth and the migration of city population over suburban areas. Besides the LI urban category, MI and HI urban area also show increasing trend from 2021 to 2031. Agricultural land and LI urban are the main contributors to MI urban and HI urban areas gain (Table 3).

Table 1. Names of 18 New Future Scenarios Generated by SWAT

Year	Name of Model								
2021	A1BLI	A1BMI	A1BHI	B1LI	B1MI	B1HI	A2LI	A2MI	A2HI
2031	A1BLI	A1BMI	A1BHI	B1LI	B1MI	B1HI	A2LI	A2MI	A2HI

Table 2. Land Cover Changes from 2011 to 2021

Land Cover*	2001 (km^2)	2011 (km^2)	2001-2011 (%)	2011-2021 LI (%)	2011-2021 MI (%)	2011-2021 HI (%)	2021-2031 LI (%)	2021-2031 MI (%)	2021-2031 HI (%)
WATR	474	478.6	1.0	0.8	0.9	0.8	0.5	0.8	0.8
URLD	2566.1	2692	4.9	9.4	4.9	4.6	17.1	4.9	4.4
URMD	405.3	437.5	7.9	8.3	7.9	7.5	9.3	8.0	7.0
URHD	173.9	182.6	5.0	5.8	5.0	9.5	7.5	5.0	8.7
SWRN	58.2	61.4	5.5	-1.0	5.6	4.1	-13.5	5.6	3.9
FRSD	9164.1	9047.8	-1.3	-1.7	-1.3	-1.3	-2.6	-1.4	-1.3
RNGE	296.4	309.1	4.3	2.7	1.7	-0.2	-0.3	4.4	3.9
HAY	3473.9	3450.4	-0.7	-1.4	-0.7	-0.7	-2.8	-0.8	-0.7
AGRR	4277.1	4210.2	-1.6	-2.8	-1.7	-1.7	-5.5	-1.9	-1.7
WETF	481.9	501.5	4.1	2.4	4.0	3.9	-0.6	4.0	3.7

* Land Cover: WATR is Open water; URLD is Low density urban; URMD is Medium density urban; URHD is High density urban; SWRN is Barren land; FRSD is Forest; RNGE is Range land; HAY is Pasture land; AGRR is Agriculture land; WETF is Wetland.

5.2. Analysis of Urban Sprawl to Land Resources

From Tables 1, 2 and 3, we can see that the newly developed urban areas are dominated by the low density urban category and the gaining areas mainly come from agricultural land. Forest is the second contributor to low density urban. The impervious surface areas in the study region are increasing corresponding to the development of medium density and high density urban categories. Forest in the study area is decreasing dramatically surrounding the urban areas. The total area of agricultural land is decreased even if it gained area from the forest lost.

According to the LRI indicators we mentioned above, the trajectories of LCLUC in the study area fulfill four conditions of the indicators even the wetland increased slightly every decade. This phenomenon implies that the St. Louis metropolitan area is undergoing urban sprawling patterns.

5.3. SWAT Model Calibration and Validation

After the sensitivity analysis, 13 parameters are ascertained to be the most sensitive for flow calibration, 6 parameters are sensitive for TSS calibration. These parameters and their best-fitted values from SUFI-2 are shown in Table 4. The best-fitted parameters are used to edit SWAT initial input, running the simulation from 2006 to 2011.

The details of model calibration and validation of flow and TSS are described in Table 5. At the end of monthly simulations, the Nash-Sutcliffe coefficients of flow in four stations were approximately equal to 0.99 while the average Nash-Sutcliffe coefficient of TSS simulation was 0.73.

5.4. Watershed Response of TSS to Climate Scenarios

In order to identify the impacts of three future climate scenarios on the TSS loading rate, we divide the results of 18 model simulations into three groups basing on the future land use scenarios, and then compute the difference of mean annual daily TSS loading at the subbasin level in three groups respectively (see Figure 4). Since the ranges of the differences between the three emission scenarios do not vary much according to the different land cover scenarios, only the LI scenario is presented in the following results. The results show that A2 characterized by high CO_2 emission with slow technological change yields higher TSS loading than scenarios A1B and B1 in most of subbasins under all land use scenarios in 2021 and 2031. The differences between A2 and A1B (Figures 4a and 4b) and between A2 and B1 (Figures 4c and 4d) present the same sub-basin distribution under the three land use scenarios of the same year, but the distribution patterns are slightly different between 2021 and 2031. The mean annual daily TSS of A1B scenarios minus scenarios B1 in 2021 and 2031 in the group LI land use scenarios are shown in Figures 4e and 4f. From the Figures 4a and 4c we can see that in A2 minus A1B and A2 minus B1 in 2021, 53 subbasins yield positive values except subbasin 4 which has a minor negative value. In 2031, in A2 minus A1B, four subbasins in the urban area yield negative value (Figure 4b), and all subbasins yield positive value when A2 subtracted by B1 (Figure 4d). Therefore, the results indicate that the TSS loading rate accompanying with future climate scenario A2 is much higher than the loading rate with scenarios A1B and B1.

The difference between A1B and B1 also has the same subbasin distribution under all land use scenarios in the same year, and slightly different between the patterns of 2021 and 2031. For the mean annual daily TSS of scenario A1B minus scenario B1, 37% of the results are negative and the rest of them are positive in 2021 (Figure 4e). In other words, 63% of

the subbasins under the climate condition of A1B scenario yield higher TSS loading rate than the yield under the condition of B1 scenario in 2021. But, in 2031, only one subbasin under the A1B scenario has lower TSS loading rate compared with the output of B1 scenario (Figure 4f). Scenario B1 characterized by low emission yields lower TSS loading rate to the river system than scenario A1B.

5.5. Watershed Response of TSS to LCLUC Scenarios

Results revealed that the TSS loading from different land cover scenarios yield different loadings in the subbasins with urban land cover. There is no obvious loading rate differences in the areas without urban cover no matter which land cover scenarios are used (Figure 5). The results are corresponding to the different land cover scenarios that have specific incentive strategy applied to.

From the comparison of results (Figure 5), we can see that 96% of subbasins in which the values of TSS loading rate of LI-MI are positive, and only two subbasins, 9 and 43, in the A2 emission scenario in the year 2021 yield negative values. The results indicate that if the low intensive urban development is encouraged in future land use planning, the loading rate of sediment would possibly be higher than the land use developing pattern from historical change trend. The results of LI-MI scenarios are all higher than the results of HI-MI scenarios in 2021 and 2031. Therefore, LI with low density urban

Table 3. Area Gained and Lost among Land Cover Categories from 2011 to 2031 (km^2)

Land Cover[a]	LI[b] Scenario									
	WATR	URLD	URMD	URHD	SWRN	FRSD	RNGE	HAY	AGRR	WETF
WATR	--	-4.0	-1.9	-1.2	-6.9	29.2	-1.3	-5.0	2.5	-4.8
URLD	4.0	--	-23.8	-11.6	22.8	234.5	27.2	142.6	314.3	45.6
URMD	1.9	23.8	--	1.2	4.0	7.4	2.0	8.3	28.8	2.8
URHD	1.2	11.6	-1.2	--	1.4	0.6	0.1	1.2	9.8	0.4
SWRN	6.9	-22.8	-4.0	-1.4	--	12.9	0.4	2.8	-1.7	-1.9
FRSD	-29.2	-234.5	-7.4	-0.6	-12.9	--	-37.9	27.0	-62.9	-30.6
RNGE	1.3	-27.2	-2.0	-0.1	-0.4	37.9	--	5.2	-7.6	0.1
HAY	5.0	-142.6	-8.3	-1.2	-2.8	-27.0	-5.2	--	36.8	3.2
AGRR	-2.5	-314.3	-28.8	-9.8	1.7	62.9	7.6	-36.8	--	-23.5
WETF	4.8	-45.6	-2.8	-0.4	1.9	30.6	-0.1	-3.2	23.5	--
Land Cover[a]	MI[b] Scenario									
	WATR	URLD	URMD	URHD	SWRN	FRSD	RNGE	HAY	AGRR	WETF
WATR	--	-1.4	-2.2	-1.3	-7.5	29.6	-1.4	-5.0	2.6	-5.1
URLD	1.4	--	-8.9	-4.2	8.2	84.0	9.8	51.1	112.6	16.3
URMD	2.2	8.9	--	1.4	4.5	8.3	2.2	9.3	32.3	3.2
URHD	1.3	4.2	-1.4	--	1.5	0.7	0.1	1.3	10.6	0.5
SWRN	7.5	-8.2	-4.5	-1.5	--	14.0	0.4	3.0	-1.6	-2.0
FRSD	-29.6	-84.0	-8.3	-0.7	-14.0	--	-40.4	26.5	-61.4	-32.5
RNGE	1.4	-9.8	-2.2	-0.1	-0.4	40.3	--	5.8	-7.4	0.1
HAY	5.0	-51.1	-9.3	-1.3	-3.0	-26.5	-5.8	--	36.4	3.2
AGRR	-2.6	-113.0	-32.3	-10.6	1.6	61.4	7.4	-36.4	--	-24.9
WETF	5.1	-16.3	-3.2	-0.5	2.0	32.5	-0.1	-3.2	24.9	--
Land Cover[a]	HI[b] Scenario									
	WATR	URLD	URMD	URHD	SWRN	FRSD	RNGE	HAY	AGRR	WETF
WATR	--	-1.3	-1.9	-2.5	-6.9	29.2	-1.3	-5.0	2.5	-4.8
URLD	1.3	--	-7.9	-7.8	7.6	78.2	9.1	47.5	104.8	15.2
URMD	1.9	7.9	--	2.4	4.0	7.4	2.0	8.3	28.8	2.8
URHD	2.5	7.8	-2.4	--	2.7	1.2	0.2	2.3	19.6	0.9
SWRN	6.9	-7.6	-4.0	-2.7	--	12.9	0.4	2.8	-1.7	-1.9
FRSD	-29.2	-78.2	-7.4	-1.2	-12.9	--	-37.9	27.0	-62.9	-30.6
RNGE	1.3	-9.1	-2.0	-0.2	-0.4	37.9	--	5.2	-7.6	0.1
HAY	5.0	-47.5	-8.3	-2.3	-2.8	-27.0	-5.2	--	36.8	3.2
AGRR	-2.5	-104.8	-28.8	-19.6	1.7	62.9	7.6	-36.8	--	-23.5
WETF	4.8	-15.2	-2.8	-0.9	1.9	30.6	-0.1	-3.2	23.5	--

[a] Land Cover: WATR is Open water; URLD is Low density urban; URMD is Medium density urban; URHD is High density urban; SWRN is Barren land; FRSD is Forest; RNGE is Range land; HAY is Pasture land; AGRR is Agriculture land; WETF is Wetland.
[b] LI is the low density urban incentive scenario; MI is the urban developing scenario with historical trend; HI is the high density urban incentive scenario.

Table 4. SWAT Sensitive Parameters and Fitted Values

Variable	Parameter Name	Description	Fitted value
Flow	ESCO. Hru	Soil evaporation compensation factor	0.935
	CN2.mgt	Curve number	35.62
	CH_N2.rte	Manning's 'n' value for main channel	0.1
	CH_K2.rte	Effective hydraulic conductivity in main channel	40
	ALPHA_BNK.rte	Baseflow alpha factor for bank storage	0.218
	SURLAG.bsn	Surface runoff lag time	20.9
	GW_REVAP.gw	Ground water revap co-efficient	0.02
	GWQMN.gw	Threshold water depth in the shallow aquifer	1.954
	GW_DELAY.gw	Groundwater delay time	201.78
	ALPHA_BF.gw	Baseflow alpha factor	0.975
	SOL_AWC.sol	Soil available water capacity	0.159
	SOL_K.sol	Saturated hydraulic conductivity	7.234
	SOL_BD.sol	Moist bulk density	0.98
TSS	SPEXP.bsn	Exponent of re-entrainment parameter for channel sediment routing	1.448
	ADJ_PKR.bsn	Peak rate adjustment factor for sediment routing in the subbasin	1.6
	SPCON.bsn	Linear re-entrainment parameter for channel sediment routing	0.009
	PRF.bsn	Peak rate adjustment factor for sediment routing in the channel	0.7
	LAT_SED.hru	Sediment concentration in lateral flow and groundwater flow	1337.5
	USLE_P.mgt	USLE support practice factor	0.52

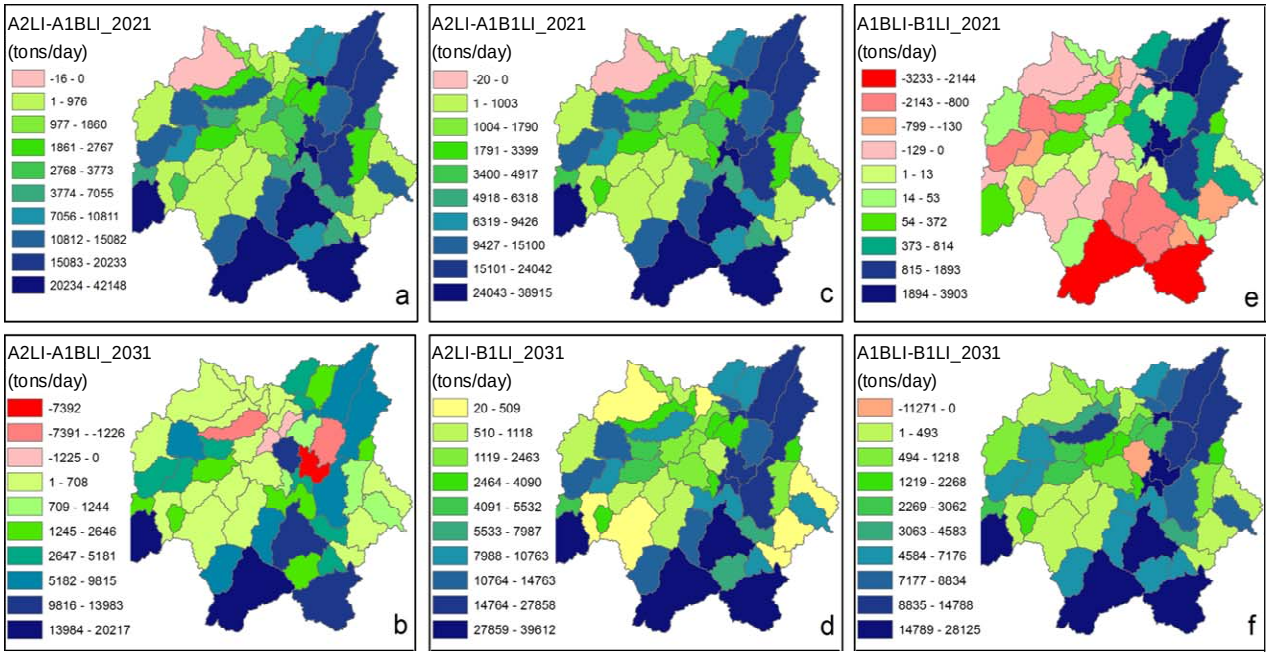

Figure 4. Differences between the mean annual daily TSS of three climate scenarios in 2021 and 2031 in the group of LI land use scenarios. The differences between A2 and A1B (Figs. 4a and 4b), between A2 and B1 (Figs. 4c and 4d), and between A1B and B1 (Fig. 4e, 4f). The TSS loading rate accompanying with future climate scenario A2 is much higher than the loading rate with scenarios A1B and B1.

incentive developing scenario may potentially cause higher TSS loading than the HI urban incentive developing pattern, and higher TSS loading than MI which has the historical urban developing pattern for the past 20 years.

The relationship between MI and HI scenarios varies in different climate scenarios and different time. In 2021, the MI scenario yields equal to or higher TSS loading than HI scenario under the A1B condition, but the opposite trend under the B1 scenario can be seen as all differences are negative. Under the A2 scenarios in 2021, three subbasins yield negative

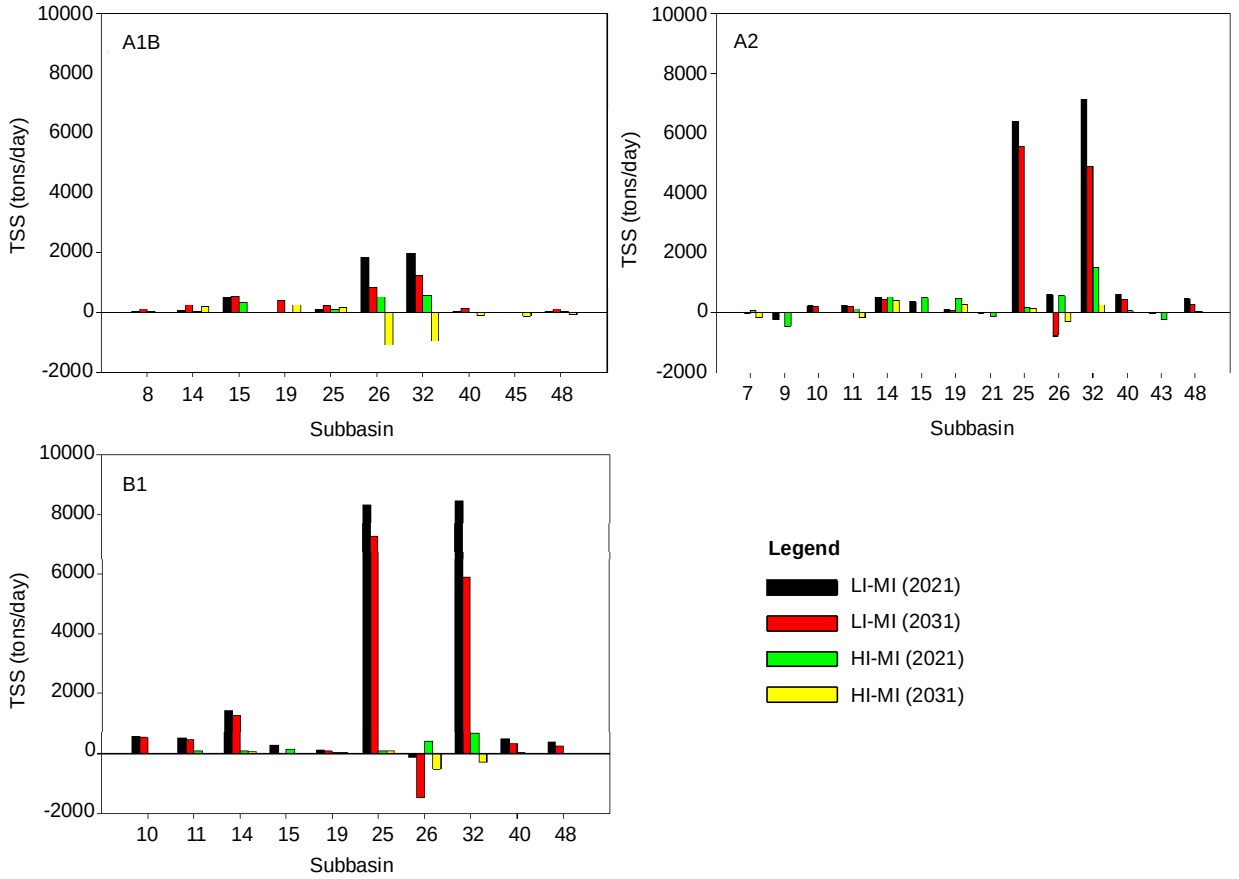

Figure 5. Average annual daily TSS of MI land cover scenario subtracted by LI and HI scenarios in the three future climate scenarios in 2021 and 2031. The results of LI-MI are positive in 96% subbasins and are all higher than the results of HI-MI scenarios in 2021 and 2031 respectively. LI land use scenario may potentially induce higher TSS loading than the HI and MI scenarios.

differences and three subbansins yield positive results, and the rest of subbasins have the same TSS loading rate in the two land change scenarios. In 2031, the differences of TSS loading rate between MI and HI land use scenarios have similar patterns in A2 and B1 climate scenarios as both land use scenarios with subbasin 2 yielding a negative value, and the rest of the values are all positive. However, in A1B emission scenario in 2031, seven subbasins of HI scenario show lower TSS loading rate than MI scenario, and three subbasins exhibit higher loading rate. From Table 2, we can see that the changing rate of high density urban area is very small even with incentive strategy. The impacts of the HI urban changes on the TSS loading can be easily compensated by the changes in other urban categories. This can be the reason why the differences in MI and HI scenarios are hard to quantify and the impacts of HI on TSS loading is difficult to predict.

In comparing the results of climate scenarios (Figure 4) versus land cover scenarios (Figure 5), it is readily evident that the magnitude of the different TSS loading rate from the different climate scenarios is much higher than those from the land cover change scenarios. One may be tempted to conclude that the impacts of climate changes on the TSS loading rate may be larger than the impacts from the land cover changes in the study area. However, this conclusion is equally arguable and requires extensive sensitivity analysis. The biggest problem is the fact that future projections use a number of assumptions that in itself bear uncertainties with various parameters settings.

Table 5. Statistics for the Model Calibration and Validation

Variables	Flow		TSS	
Stations	Calibration	Validation	Calibration	Validation
Below Grafton	R^2: 0.99	R^2: 0.99	R^2: 0.83	R^2: 0.67
	NS: 0.99	NS: 0.99	NS: 0.65	NS: 0.61
St. Charles	R^2: 0.99	R^2: 0.99	R^2: 0.76	R^2: 0.83
	NS: 0.99	NS: 0.99	NS: 0.66	NS: 0.71
St. Louis	R^2: 0.99	R^2: 0.99	R^2: 0.87	R^2: 0.87
	NS: 0.99	NS: 0.99	NS: 0.81	NS: 0.86
Chester	R^2: 0.99	R^2: 0.99	R^2: 0.79	R^2: 0.83
	NS: 0.99	NS: 0.99	NS: 0.76	NS: 0.81

Table 6. Average Annual Daily TSS Loading Rate and Percentage of Low Density Urban Area between LI and MI in 2021 and 2031

Subbasin	Area (km^2)	% of URLD[a] (LI)[b]	% of URLD (MI)[b]	% difference of URLD	LI-MI A1B (tons/d)	LI-MI A2 (tons/d)	LI-MI B1 (tons/d)
				2021			
14	136	68.4	65.6	2.8	35	533	70
15	421	35.3	33.8	1.4	483	488	133
19	445	43.6	41.8	1.8	4	471	16
25	285	82.0	78.6	3.3	78	188	87
26	271	28.6	27.4	1.2	1842	582	390
31	96	61.5	59.0	2.5	1	15	2
32	118	30.5	29.2	1.2	1958	1533	675
40	406	13.5	13.0	0.6	22	67	8
				2031			
14	136	80.1	68.9	11.3	251	506	1440
15	421	41.3	35.5	5.8	543	381	293
19	445	51.0	43.8	7.2	382	102	103
25	285	96.0	82.5	13.5	208	6384	8336
26	271	33.5	28.7	4.7	825	600	-117
31	96	72.0	61.9	10.1	7	75	95
32	118	35.7	30.7	5.0	1233	7142	8467
40	406	15.8	13.6	2.2	133	618	492

[a] URLD is low density urban land cover.
[b] LI is the low density urban incentive scenario; MI is the urban developing scenario with historical trend.

Table 7. Percentage of Agricultural Land in LI and MI in 2021 and 2031

Subbasins[a]	% of AGRR[b] (LI)[c]	% of AGRR (MI)[c]	% of AGRR (LI)	% of AGRR (MI)
	2021		2031	
14	7.7	7.7	7.2	7.5
15	17.1	17.3	16.2	16.8
19	20.4	20.6	19.3	20.0
25	0.0	0.0	0.0	0.0
26	25.9	26.2	24.5	25.5
31	0.4	0.4	0.4	0.4
32	22.0	22.3	20.8	21.7
40	27.1	27.4	25.6	26.7

[a] Subbasins here only include those having different average annual daily TSS loading rate under different land cover scenarios.
[b] AGRR is agriculture land.
[c] LI is the low density urban incentive scenario; MI is the urban developing scenario with historical trend.

5.6. Correlation Analysis between TSS Loading and Urban Area

As shown in Figure 5, TSS loading expressed by the difference between LI scenarios and MI scenarios are positive for the 96% of the subbasins, and generally higher than the results of the HI scenarios subtracted by MI scenarios. This implies that the LI may cause a higher TSS loading compared to the other two LCLUC scenarios in all future climate conditions. In order to identify the correlation between TSS loading rate and urban developing patterns, we select eight subbasins which have variable TSS loading rate in different climate scenarios, and plot the differences of TSS loading rate with the low density urban area of LI and MI scenarios (Table 6). A common feature of these eight subbasins is the high percentage of the low density urban area (i.e., the percentage of seven subbasins are all higher than 27%), and only one subbasin has a lower percentage but still above 13%. The percentages of low density urban area of each subbasin in LI are all higher than in MI in 2021 and 2031 and the percentage difference between LI and MI in 2031 is increasing compared with 2021. But from Table 6, we also notice that the magnitude of different TSS loading rate between the land cover scenarios and the changing trends of TSS loading rate from 2021 to 2031 are not consistent with the percentage of low density urban change in the subbasins. This is an indication that different land cover scenarios have different TSS loading rate in these subbasins with high low density urban area cover, but the magnitude of different TSS loading rate does not depend on

the percentage of low density urban cover area.

We list the percentage of agricultural land of the subbasins having different average annual daily TSS loading rate under different land cover scenarios in Table 7. The magnitude of different TSS loading rate in Table 6 corresponds to the percentage of agricultural land in Table 7. For example, the higher the percentage of the agriculture land, the larger the TSS loading rate and the different land cover scenarios, or vice versa. The areas with high low density urban land cover of LI is related to higher TSS loading rate than MI and HI and the source of TSS is mainly from agricultural land.

The results in this section indicated that when the low density urban is encouraged to develop with a higher growing rate (LI), the runoff may potentially increase compared to the MI with the historical urban development patterns. The incentive of high density urban development of MI scenario also impacts the runoff, but not as much as the impacts from LI. When runoff increases, more TSS is carried by the runoff and loaded into the rivers.

6. Conclusions

This paper developed a general model of the implications of climate change and land use modifications to the water quality in the St. Louis metropolitan regions. The outcome of this study is useful in identifying the effects of LCLUC characterized by rapid suburbanization and depopulation of urban core on water resources.

The results revealed that the future climate variability and land cover changes may have potential impacts on the suspended sediment loading into the surface waters at the confluence of Mississippi River, Missouri River, and Illinois River. The impacts from climate changes would be much severe than from urban expansion based on the simulation results of the three climate change scenarios. The A2 emission climate scenario characterized by high CO_2 emission with slow technological change yields significantly higher TSS loading rate in the research area.

The impacts of land cover changes on the TSS loading rate is smaller than the impacts from climate change, but it is still noticeable in subbasin scale. The LI scenario with high development of low density urban area yielded higher TSS contaminant to the water body than another two land cover scenarios. The results also indicated the primary contributor of TSS loading rate increase is the forest lost and urban expansion, and the TSS contaminant is mainly came from agricultural land. We conclude that the urban sprawl developing pattern accompanied by deforestation increase the surface runoff which can cause heavier erosion in the agriculture land and transport higher amount of suspended sediment into the river. The loading of anthropogenic fertilizers superimposed on the suspended sediment from agriculture can further accelerate water quality deterioration.

This study presented a methodology to predict the changes in the sediment load from the study area which is expected to impact the water quality of the three important rivers. However, the uncertainties of the model outputs were not quantified due to data limitations. The specific location of study site at a confluence of larger rivers may be associated with causality of simulation uncertainties and errors in model calibration. There is a big channel band at the upper section of the confluence of the Mississippi River and Illinois River. This big band can reduce the flow velocity thereby increasing settling velocity of sediments. The Melvin Price Locks and Dam located above the confluence of Missouri and Mississippi River can also be a potential factor that contribute sediment transport downstream. In addition, the sediment from the impervious surfaces cannot be measured and simulated accurately. All these factors may have brought additional uncertainties to our results. Additional study that will quantify these uncertainties are deemed recommended.

Acknowledgments. Landsat data is courtesy of U.S. Geological Survey. The Center for Environmental Sciences at Saint Louis University is an ITT Geospatial Innovation Center. ENVI is a registered trademark of ITT Visual Information Solutions, Incorporated. Authors would like to thank anonymous reviewers for their constructive comments.

References

Abbaspour, K.C., Faramarzi, M., Ghasemi, S.S., and Yang, H. (2009). Assessing the impact of climate change on water resources in Iran. *Water Resour. Res.,* 45(10), W10434. http://dx.doi.org/10.1029/2008WR007615

Abbaspour, K.C., Johnson, C.A., and Van Genuchten, M.T. (2004). Estimating uncertain flow and transport parameters using a sequential uncertainty fitting procedure. *Vadose Zone J.,* 3(4), 1340-1352. http://dx.doi.org/10.2113/3.4.1340

Abbaspour, K.C., Yang, J., Maximov, I., Siber, R., Bogner, K., Mieleitner, J., Zobrist, J., and Srinivasan, R. (2007). Modelling hydrology and water quality in the pre-ailpine/alpine Thur watershed using SWAT. *J. Hydrol.,* 333(2-4), 413-430. http://dx.doi.org/10.1016/j.jhydrol.2006.09.014

Anderson, J.R., Hardy, E.E., Roach, J.T., and Witmer, R.E. (1976). *A Land Use and Land Cover Classification System for Use with Remote Sensor Data,* United States Government Printing Office, Washington, D.C.

Arnell, N.W., Hudson, D.A., and Jones, R.G. (2003). Climate change scenarios from a regional climate model: Estimating change in runoff in southern Africa. *J. Geophys. Res. (D Atmos.) (1984-2012),* 108(D16), 4519. http://dx.doi.org/10.1029/2002JD 002782

Arnold, J.G., Allen, P.M., Volk, M., Williams, J.R., and Bosch, D.D. (2010). Assessment of different representations of spatial variability on SWAT model performance. *Trans. ASABE,* 53(5), 1433-1443. http://dx.doi.org/10.13031/2013.34913

Arnold, J.G., Srinivasan, R., Muttiah, R.S., and Williams, J.R. (1998). Large area hydrologic modeling and assessment-Part 1: Model development. *J. Am. Water Resour. Assoc.,* 34, 73-89. http://dx.doi.org/10.1111/j.1752-1688.1998.tb05961.x

Bernstein, L.S., Adler-Golden, S.M., Sundberg, R.L., Levine, R.Y., Perkins, T.C., Berk, A., Ratkowski, A.J., Felde, G., and Hoke, M.L. (2005). Validation of the QUick Atmospheric Correction (QUAC) algorithm for VNIR-SWIR multi-and hyperspectral imagery, in S.S.L. Shen and E. Paul (Eds.), *Proc. SPIE 5806, Algorithms and Technologies for Multispectral, Hyperspectral, and Ultraspectral Imagery XI,* pp. 668-678. http://dx.doi.org/10.1117/12.603359

Box, G.E.P., and Jenkins, G.M. (1970). *Time Series Analysis:*

Forecasting and Control, Holden-Day, San Francisco.

Burn, D.H. (1994). Hydrologic effects of climatic change in west-central Canada. *J. Hydrol.,* 160(1-4), 53-70. http://dx.doi.org/10.1016/0022-1694(94)90033-7

Caballero, Y., Voirin-Morel, S., Habets, F., Noilhan, J., LeMoigne, P., Lehenaff, A., and Boone, A. (2007). Hydrological sensitivity of the Adour-Garonne River basin to climate change. *Water Resour. Res.,* 43(7), W07448. http://dx.doi.org/10.1029/2005WR004192

Callan, S.J., and Thomas, J.M. (2012). *Environmental Economics and Management: Theory, Policy, and Applications,* 6 edn., South-Western College Pub.

Callender, E., and Rice, K.C. (2000). The urban environmental gradient: anthropogenic influences on the spatial and temporal distributions of lead and zinc in sediments. *Environ. Sci. Technol.,* 34(2), 232-238. http://dx.doi.org/10.1021/es990380s

Chang, H. (2003). Basin hydrologic response to changes in climate and land use: The Conestoga River basin, Pennsylvania. *Phys. Geogr.,* 24(3), 222-247. http://dx.doi.org/10.2747/0272-3646.24.3.222

Chang, H. (2004). Water quality impacts of climate and land use changes in southeastern Pennsylvania. *Prof. Geogr.,* 56(2), 240-257.

Chen, J.F., Li, X.B., and Zhang, M. (2005). Simulating the impacts of climate variation and land-cover changes on basin hydrology: A case study of the Suomo basin. *Sci. China Ser. D (Earth Sci.),* 48(9), 1501-1509. http://dx.doi.org/10.1360/03yd0269

Choi, W. (2008). Catchment-scale hydrological response to climate-land-use combined scenarios: A case study for the Kishwaukee River basin, Illinois. *Phys. Geogr.,* 29(1), 79-99. http://dx.doi.org/10.2747/0272-3646.29.1.79

Clifford, N.J. (2009). Globalization: A physical geography perspective. *Prog. Phys. Geogr.,* 33(1), 5-16. http://dx.doi.org/10.1177/0309133309105035

Committee on Missouri River Ecosystem Science, and National Research Council (2002). *The Missouri River Ecosystem: Exploring the Prospects for Recovery,* National Academy Press, Washington, D.C.

Criss, R.E., and Wilson, D.A. (2003). *At the Confluence: Rivers, Floods, and Water Quality in the St. Louis Region,* Missouri Botanical Garden Press, St. Louis.

Davis Todd, C.E., Goss, A.M., Tripathy, D., and Harbor, J.M. (2007). The effects of landscape transformation in a changing climate on local water resources. *Phys. Geogr.,* 28(1), 21-36. http://dx.doi.org/10.2747/0272-3646.28.1.21

Deletic, A. (1998). The first flush load of urban surface runoff. *Water Res.,* 32(8), 2462-2470. http://dx.doi.org/10.1016/S0043-1354(97)00470-3

Dierberg, F.E. (1991). Non-point source loadings of nutrients and dissolved organic carbon from an agricultural suburban watershed in east central Florida. *Water Res.,* 25(4), 363-374. http://dx.doi.org/10.1016/0043-1354(91)90073-Y

Dissmeyer, G.E. (2000). Drinking water from forests and grasslands: A synthesis of the scientific literature. *Gen. Tech. Rep. SRS-39, USDA For. Serv. S. Res. Stn.,* Asheville, NC, 246.

Dreher, D.W., and Price, T.H. (1992). *Best Management Practice Handbook for Urban Development,* Northeastern Illinois Planning Commission, Chicago, IL.

Ducharne, A., Baubion, C., Beaudoin, N., Benoit, M., Billen, G., Brisson, N., Garnier, J., Kieken, H., Lebonvallet, S., Ledoux, E., Mary, B., Mignolet, C., Poux, X., Sauboua, E., Schott, C., Théry, S., and Viennot, P. (2007). Long term prospective of the Seine River system: Confronting climatic and direct anthropogenic changes. *Sci. Total Environ.,* 375(1-3), 292-311. http://dx.doi.org/10.1016/j.scitotenv.2006.12.011

ERDAS (ed) (1999). *ERDAS Field Guide™,* ERDAS Inc., Atlanta, Georgia.

Franczyk, J., and Chang, H. (2009). The effects of climate change and urbanization on the runoff of the Rock Creek basin in the Portland metropolitan area, Oregon, USA. *Hydrol. Process.,* 23(6), 805-815. http://dx.doi.org/10.1002/hyp.7176

Frederick, K.D., and Schwarz, G.E. (1999). Socioeconomic impacts of climate change on US water supplies. *J. Am. Water Resour. Assoc.,* 35(6), 1563-1583. http://dx.doi.org/10.1111/j.1752-1688.1999.tb04238.x

Frumkin, H. (2002). Urban sprawl and public health. *Public Health Rep.,* 117(3), 201-217. http://dx.doi.org/10.1016/S0033-3549(04)50155-3

Fu, G., Charles, S.P., Viney, N.R., Chen, S.L., and Wu, J.Q. (2007). Impacts of climate variability on stream-flow in the Yellow River. *Hydrol. Process.,* 21(25), 3431-3439. http://dx.doi.org/10.1002/hyp.6574

Goonetilleke, A., Thomas, E., Ginn, S., and Gilbert, D. (2005). Understanding the role of land use in urban stormwater quality management. *J. Environ. Manage.,* 74(1), 31-42. http://dx.doi.org/10.1016/j.jenvman.2004.08.006

Hasse, J.E., and Lathrop, R.G. (2003). Land resource impact indicators of urban sprawl. *Appl. Geogr.,* 23(2), 159-175. http://dx.doi.org/10.1016/j.apgeog.2003.08.002

Hepinstall, J.A., Alberti, M., and Marzluff, J.M. (2008). Predicting land cover change and avian community responses in rapidly urbanizing environments. *Landscape Ecol.,* 23(10), 1257-1276. http://dx.doi.org/10.1007/s10980-008-9296-6

Ierodiaconou, D., Laurenson, L., Leblanc, M., Stagnitti, F., Duff, G., and Salzman, S. (2004). Multi-temporal land use mapping using remotely sensed techniques and the integration of a pollutant load model in a GIS. *IAHS Publ.,* 289, 343-352.

Immergluck, D. (2010). Neighborhoods in the wake of the debacle: Intrametropolitan patterns of foreclosed properties. *Urban Aff. Rev.,* 46(1), 3-36. http://dx.doi.org/10.2139/ssrn.1533786

Ingram, J.C., Dawson, T.P., and Whittaker, R.J. (2005). Mapping tropical forest structure in southeastern Madagascar using remote sensing and artificial neural networks. *Remote Sens. Environ.,* 94(4), 491-507. http://dx.doi.org/10.1016/j.rse.2004.12.001

Intergovernmental Panel on Climate Change (IPCC) (2000). *Special Report on Emissions Scenarios (SRES),* in N. Nakicenovic, and R. Swart (Eds.), A Special Report of Working Group III of the Intergovernmental Panel on Climate Change, Cambridge University Press, Cambridge.

Intergovernmental Panel on Climate Change (IPCC) (2007). *Impacts, Adaptation and Vulnerability,* in M.L. Parry, O.F. Canziani, J.P. Palutikof, P.J. van der Linden, and C.E. Hanson (Eds.), Contribution of Working Group II to the Fourth Assessment Report of the Intergovernmental Panel on Climate Change, Cambridge University Press, Cambridge.

Jensen, J.R. (1996). *Introductory Digital Image Processing: A Remote Sensing Perspective,* Prentice-Hall Inc., Upper Saddle River, New Jersey, 225-229.

Jha, M., Gassman, P.W., Secchi, S., Gu, R., and Arnold, J. (2004a). Effect of watershed subdivision on swat flow, sediment, and nutrient predictions. *J. Am. Water Resour. Assoc.,* 40(3), 811-825. http://dx.doi.org/10.1111/j.1752-1688.2004.tb04460.x

Jha, M., Pan, Z.T., Takle, E.S., and Gu, R. (2004b). Impacts of climate change on streamflow in the Upper Mississippi River basin: A regional climate model perspective. *J. Geophys. Res. (D Atmos.),* 109(D09). http://dx.doi.org/10.1029/2003JD003686

Jha, M.K. (2011). Evaluating hydrologic response of agricultural watershed for watershed analysis. *Water,* 3, 14. http://dx.doi.org/10.3390/w3020604

Jordan, Y.C., Ghulam, A., and Herrmann, R.B. (2012). Floodplain ecosystem response to climate variability and land-cover and land-use change in Lower Missouri River basin. *Landscape Ecol.,* 27(6), 843-857. http://dx.doi.org/10.1007/s10980-012-9748-x

Jyrkama, M.I., and Sykes, J.F. (2007). The impact of climate change on spatially varying groundwater recharge in the Grand River watershed (Ontario). *J. Hydrol.,* 338(3), 237-250. http://dx.doi.org/10.1016/j.jhydrol.2007.02.036

Leopold, L.B. (1968). *Hydrology for Urban Land Planning: A Guidebook on the Hydrological Effects of Urban Land Use,* U.S. Geological Survey, Washington, D.C.

Liang, S.H., Ge, S.M., Wan, L., and Xu, D.W. (2012). Characteristics and causes of vegetation variation in the source regions of the Yellow River, China. *Int. J. Remote Sens.,* 33(5), 1529-1542. http://dx.doi.org/10.1080/01431161.2011.582187

Lopez, E., Bocco, G., Mendoza, M., and Duhau, E. (2001). Predicting land-cover and land-use change in the urban fringe: A case in Morelia city, Mexico. *Landscape Urban Plann.,* 55(4), 271-285. http://dx.doi.org/10.1016/S0169-2046(01)00160-8

Luenberger, D.G. (1979). *Introduction to Dynamic Systems: Theory, Models, and Applications.* 1 edn, New York, Wiley.

Manakos, I., Liebler, J., and Schneider, T. (2000). Parcel based calibration of remote sensing data for precision farming purposes, *in: Angewandte Geographische Informationsverarbeitung XII,* Salzburg, Austria, pp. 333-344.

Maurer, E.P., Brekke, L., Pruitt, T., and Duffy, P.B. (2007). Fine-resolution climate projections enhance regional climate change impact studies. *Eos, Trans. AGU,* 88(47), 504. http://dx.doi.org/10.1029/2007EO470006

Mimikou, M.A., Baltas, E., Varanou, E., and Pantazis, K. (2000). Regional impacts of climate change on water resources quantity and quality indicators. *J. Hydrol.,* 234(1), 95-109. http://dx.doi.org/10.1016/S0022-1694(00)00244-4

Missouri Department of Natural Resources (MDNR) (2012). Major water users-Data. *Water Resour. Cent.,* http://www.dnr.mo.gov/env/wrc/mwudata.htm (accessed on March 2012)

Mortsch, L.D., and Quinn, F.H. (1996). Climate change scenarios for Great Lakes basin ecosystem studies. *Limnol. Oceanogr.,* 41, 903-911. http://dx.doi.org/10.4319/lo.1996.41.5.0903

Nash, J.E., and Sutcliffe, J.V. (1970). River flow forecasting through conceptual models part I-A discussion of principles. *J. Hydrol.,* 10(3), 282-290. http://dx.doi.org/10.1016/0022-1694(70)90255-6

National Land Cover Database (NLCD) (2012). Multi-Resolution Land Characteristics Consortium (MRLC), http://www.mrlc.gov/nlcd06_data.php. (accessed on March 2012)

National Oceanic and Atmospheric Administration (NOAA) (2012). National Climatic Data Center, http://www.ncdc.noaa.gov/. (accessed on March 2012)

Noble, C. (1999). Lifeline for a landscape: Baltimore-Washington area. *Am. For.,* 105, 3.

Nunes, J.P., Seixas, J., Keizer, J.J., and Ferreira, A.J.D. (2009). Sensitivity of runoff and soil erosion to climate change in two Mediterranean watersheds. Part I: model parameterization and evaluation. *Hydrol. Process.,* 23(8), 1202-1211. http://dx.doi.org/10.1002/hyp.7247

Pan, Z.T., Arritt, R.W., Takle, E.S., Gutowski, W.J., Anderson, C.J., and Segal, M. (2004). Altered hydrologic feedback in a warming climate introduces a "warming hole". *Geophys. Res. Lett.,* 31, L17109. http://dx.doi.org/10.1029/2004GL020528

Phillips, N. J., and Lewis, E. T. (1995). Site planning from a watershed perspective, *in: National conference on urban runoff management: Enhancing urban watershed management at the local, county, and State levels (Eds.),* Environmental Protection Agency, Office of Research and Development, Center for Environmental Research Information, Cincinnati, U.S., pp. 135-150.

Pimentel, D. (2000). Soil erosion and the threat to food security and the environment. *Ecosyst. Health,* 6(4), 221-226. http://dx.doi.org/10.1046/j.1526-0992.2000.006004221.x

Randhir, T.O., and Hawes, A.G. (2009). Watershed land use and aquatic ecosystem response: Ecohydrologic approach to conservation policy. *J. Hydrol.,* 364(1), 182-199. http://dx.doi.org/10.1016/j.jhydrol.2008.10.017

Samaniego, L., and Bardossy, A. (2006). Simulation of the impacts of land use/cover and climatic changes on the runoff characteristics at the mesoscale. *Ecol. Model.,* 196(1), 45-61. http://dx.doi.org/10.1016/j.ecolmodel.2006.01.005

Scibek, J., and Allen, D.M. (2006). Modeled impacts of predicted climate change on recharge and groundwater levels. *Water Resour. Res.,* 42(11), W11405. http://dx.doi.org/10.1029/2005WR004742

Singh, V.P., and Xu, Y.J. (2006). Coastal hydrology and processes, *in the AIH 25th Anniversary Meeting & International Conference "Challenges in coastal Hydrology and Water Quality" (Eds.),* Water Resources Publications LLC, Highlands Ranch, Colorado, U.S., pp. 105.

Sonzogni, W.C., Chesters, G., Coote, D.R., Jeffs, D.N., Konrad, J.C., Ostry, R.C., and Robinson, J.B. (1980). Pollution from land runoff. *Environ. Sci. Techno.,* 14(2), 148-153. http://dx.doi.org/10.1021/es60162a003

Stephenson, D. (1994). Comparison of the water balance for an undeveloped and a suburban catchment. *J. Hydrol. Sci.,* 39(4), 295-307. http://dx.doi.org/10.1080/02626669409492751

Stone, M.C., Hotchkiss, R.H., and Mearns, L.O. (2003). Water yield responses to high and low spatial resolution climate change scenarios in the Missouri River basin. *Geophys. Res. Lett.,* 30(4), 1186. http://dx.doi.org/10.1029/2002GL016122

Thomas, D.S.G., Twyman, C., Osbahr, H., and Hewitson, B. (2007). Adaptation to climate change and variability: farmer responses to intra-seasonal precipitation trends in South Africa. *Clim. Change.,* 83(3), 301-322. http://dx.doi.org/10.1007/s10584-006-9205-4

Tiao, G.C., and Box, G.E.P. (1981). Modeling multiple time series with applications. *J. Am. Stat. Assoc.,* 76 (376), 802-816.

U.S. Department of Agriculture (USDA) (2012). *SPELLmap, Unreleased software,* Grazinglands Research Laboratory, United States Department of Agriculture-Agricultural Research Services, El Reno, Oklahoma.

U.S. Geological Survey (USGS) (2012a). National Elevation Dataset (NED), edited. http://nationalmap.gov/viewer.html. (accessed on March 2012)

U.S. Geological Survey (USGS) (2012b). Water watch, current streamflow, edited. http://waterwatch.usgs.gov/?m=real&r=mo&w=map. (accessed on March 2012)

Van Metre, P.C., Mahler, B.J., and Furlong, E.T. (2000). Urban sprawl leaves its PAH signature. *Environ. Sci. Technol.,* 34(19), 4064–407. http://dx.doi.org/10.1021/es991007n

Wang, Y., Choi, W., and Deal, B.M. (2005). Long-term impacts of land-use change on non-point source pollutant loads for the St. Louis metropolitan area, USA. *Environ. Manage.,* 35(2), 194-205. http://dx.doi.org/10.1007/s00267-003-0315-8

Weng, Q.H. (2001). Modeling urban growth effects on surface runoff with the integration of remote sensing and GIS. *Environ. Manage.,* 28(6), 737-748. http://dx.doi.org/10.1007/s002670010258

Wilby, R.L., Whitehead, P.G., Wade, A.J., Butterfield, D., Davis, R.J., and Watts, G. (2006). Integrated modelling of climate change impacts on water resources and quality in a lowland catchment: River Kennet, UK. *J. Hydrol.,* 330(1), 204-220. http://dx.doi.org/10.1016/j.jhydrol.2006.04.033

Wilson, C.O., and Weng, Q.H. (2011). Simulating the impacts of

future land use and climate changes on surface water quality in the Des Plaines River watershed, Chicago Metropolitan Statistical Area, Illinois. *Sci. Total Environ.,* 409(20), 4387-4405. http://dx.doi.org/10.1016/j.scitotenv.2011.07.001

Woodcock, C.E., Macomber, S.A., Pax-Lenney, M., and Cohen, W.B. (2001). Monitoring large areas for forest change using Landsat: Generalization across space, time and Landsat sensors. *Remote Sens. Environ.,* 78(1), 194-203. http://dx.doi.org/10.1016/S0034-4257(01)00259-0

Wu, Q., Li, H.Q., Wang, R.S., Paulussen, J., He, Y., Wang, M., Wang, B.H., and Wang, Z. (2006). Monitoring and predicting land use change in Beijing using remote sensing and GIS. *Landscape Urban Plann.,* 78(4), 322-333. http://dx.doi.org/10.1016/j.landurbplan.2005.10.002

Xiong, K.G., Yang, J., Wan, S.Q., Feng, G.L., and Hu, J.G. (2009). Monte Carlo simulation of the record-breaking high temperature events of climate changes. *Acta Phys. Sin.,* 58, 2843-2852.

Young, W.J., Marston, F.M., and Davis, J.R. (1996). Nutrient exports and land use in Australian catchments. *J. Environ. Manage.,* 47(2), 165-183. http://dx.doi.org/10.1006/jema.1996.0043